POLITECNICO DI TORINO
Repository ISTITUZIONALE

A static analysis of three-dimensional sandwich beam structures by hierarchical finite elements modelling

Publisher copyright

(Article begins on next page)

04 August 2020

A static analysis of three-dimensional sandwich beam structures by hierarchical finite elements modelling

Gabriele De Pietro[1] [2], Gaetano Giunta[1], Salim Belouettar[1] and Erasmo Carrera[2]

Abstract

A static analysis of three-dimensional sandwich beam structures using one-dimensional modelling approach is presented within this paper. A family of several one-dimensional beam elements is obtained by hierarchically expanding the displacements over the cross-section and letting the expansion order a free parameter. The finite element approximation order over the beam axis is also a formulation free parameter (linear, quadratic and cubic elements are considered). The principle of virtual displacements is used to obtain the problem weak form and derive the beam stiffness matrix and equivalent load vectors in a nuclear, generic form. Displacements and stresses are presented for different load and constraint configurations. Results are validated towards three-dimensional FEM solutions and experimental results. Sandwich beams present a three-dimensional stress state and higher-order models are necessary for an accurate description. Numerical investigations show that fairly good results with reduced computational costs can be obtained by the proposed finite element formulation.

Keywords

Three-dimensional beams, static analysis, finite element solution, one-dimensional hierarchical theories, mechanics of sandwich structures

[1] Luxembourg Institute of Science and Technology, 5, avenue des Hauts-Fourneaux, L-4362 Esch-sur-Alzette, Luxembourg
[2] Politecnico di Torino, c.so Duca degli Abruzzi, 24, 10129, Turin, Italy

Corresponding author:
Gabriele De Pietro, Materials Research and Technology Department, Luxembourg Institute of Science and Technology, 5, avenue des Hauts-Fourneaux, L-4362 Esch-sur-Alzette, Luxembourg. tel: +352 275 888 1.
Email: gabriele.depietro@list.lu

Introduction

Due to their high stiffness-to-weight and strength-to-weight ratios, sandwich structures are more and more used in industry as light weight structural elements. The great difference in stiffness between the face sheets and the core makes the prediction of the mechanical behaviour of such structures very challenging. It is well established that classical models are generally inadequate for the analysis of sandwich beams since the cross-section is considered to be rigid on its own plane and displacements occurring in the soft core can not be accounted for. Higher-order models are, therefore, needed in order to accurately predict the displacement and stress fields. For these reasons, sandwich beams modelling is an up-to-date research field.

One of the first examples of sandwich structures used in civil engineering can be found in Fairbairn [1] whereas a first general tractation was provided by Allen [2]. A general overview on modelling of sandwich structures can be found in Noor et al. [3] and Librescu and Terry [4]. Classical equivalent single layer Euler-Bernoulli's and Timoshenko's models can be improved by using a different displacement field for the core and the skins. Krajcinovic [5] carried out the static analysis of a sandwich beam by assuming Euler-Bernoulli's kinematic hypothesis independently for each lamina. Banerjee and Sobey [6] used Rayleigh's and Timoshenko's kinematics for the skins and core, respectively. Damanpack and Khalili [7] used cubic and quadratic polynomials in the through-the-thickness coordinate in the core for the axial and transverse displacement components, whereas the skins were modelled according to Euler-Bernoulli's theory. Léotoing at al. [8] assumed a cubic and a quadratic expansion for the core displacement components as well as linear and constant axial and transverse displacements for the skins. Frostig et al. [9, 10] carried out a static analysis of sandwich beams accounting for local effects by using a beam theory for the skins and a two-dimensional elasticity theory for the core. Cho and Averill [11] proposed a new one-dimensional finite element with sublaminate first-order zig-zag kinematic assumptions to study laminated beams with low and high aspect ratios. Kapuria et al. [12] carried out static, buckling and free as well as forced vibration analyses adopting a third-order zig-zag theory. The effect of the scale of the basic core cell in the static response of sandwich beams was investigated by Dai and Zhang [13]. Vidal and Polit [14] formulated a family of sinus-refined finite beam elements. Hu et al. [15] used several layer-wise models to study the stability of sandwich beams. Hu et al. [16] studied instabilities in sandwich structures using Léotoing at al. [8] kinematics and the finite element method. Stemming from the kinematics of Phan et al. [17], Wang and Wang [18] formulated a weak form quadrature sandwich beam element. Pourvais et al. [19] numerically and experimentally investigated sandwich beams accounting for localised effects due to a high difference in stiffness between the core and the skin face sheets. By means of Jourawski's method, Bardella and Mattei [20] obtained an explicit analytical solution accounting for zig-zag warping. Salami et al. [21] presented an advanced high-order sandwich panel theory for bending analysis of moderately thick beams. Ritz method was adopted to derive the governing equations and geometrical non-linearity in the face sheets were accounted for.

Stemming from the work done on composites plates and shells, see Carrera [22], Carrera and Giunta [23, 24] and Giunta et al. [25, 26], a Unified Formulation (UF) for the static analysis of three-dimensional sandwich beams is presented in this paper. Through this formulation, non-classical higher-order deformations such as in- and out-of-plane warping are accounted for, see Carrera et al. [27], Giunta et al [28], Catapano et al. [29] and He et al. [30]. Furthermore, classical Euler-Bernoulli's (EBT) and Timoshenko's (TBT) models are obtained as special cases. As far as sandwich beams are concerned, UF was used in the framework of a Navier-type solution, see Giunta et al. [31]. The novelty of the

present work consists in the use of the finite element method to solve the problem in a weak sense. The stiffness matrix is, therefore, obtained through the principle of virtual displacements in the form of a fundamental nucleus that is not dependent upon the order of expansion of the displacement field as well as the number of nodes per element. Shear locking is corrected by a classical selective integration procedure, see Bathe [32], that is effective regardless the approximation order over the cross-section. Analyses are carried out for different length-to-thickness ratios. Slender and very short beams are investigated. In particular, the accuracy and the limit of the proposed models are thoroughly investigated by considering very challenging problems governed by a complex three-dimensional stress state (bending, torsion as well as localised effects) and a high material anisotropy ratio between skins and core. Results are provided in terms of displacements and stresses. The proposed models are validated through comparison with three-dimensional finite element solutions obtained by Ansys showing that fairly accurate results can be obtained with reduced computational costs.

Displacement Field Approximation

A Cartesian reference system is adopted, see Fig. 1: the x coordinate is aligned with the direction of the longitudinal axis of the beam, y- and z-axis are two orthogonal directions laying on the plane of the cross-section Ω. The displacement vector is:

$$\mathbf{u}^T(x, y, z) = \left\{ \begin{array}{ccc} u_x(x, y, z) & u_y(x, y, z) & u_z(x, y, z) \end{array} \right\}, \tag{1}$$

where u_x, u_y and u_z are the components along x-, y- and z-axis and superscript 'T' represents the transposition operator.

The displacement field is a priori assumed over the cross-section in the following manner:

$$\mathbf{u}(x, y, z) = F_\tau(y, z)\,\mathbf{u}_\tau(x) \quad \text{with} \ \tau = 1, 2, \ldots, N_u \tag{2}$$

According to Einstein's notation, subscript τ implicitly represents a summation. $F_\tau(y, z)$ is a generic expansion function over the cross-section and N_u is the number of the accounted terms.

This kinematic formulation allows to derive several beam theories being the choice of the expansion functions $F_\tau(y, z)$ and N_u arbitrary. In this study, Mac Laurin's polynomials are used as approximating functions. N_u and F_τ as function of the order of the theory N are obtained through Pascal's triangle as shown in Table 1.

The explicit form of a generic N-order displacement field is:

$$\begin{aligned}
u_x &= u_{x1} + u_{x2}y + u_{x3}z + \cdots + u_{x\frac{(N^2+N+2)}{2}}y^N + \cdots + u_{x\frac{(N+1)(N+2)}{2}}z^N, \\
u_y &= u_{y1} + u_{y2}y + u_{y3}z + \cdots + u_{y\frac{(N^2+N+2)}{2}}y^N + \cdots + u_{y\frac{(N+1)(N+2)}{2}}z^N, \\
u_z &= u_{z1} + u_{z2}y + u_{z3}z + \cdots + u_{z\frac{(N^2+N+2)}{2}}y^N + \cdots + u_{z\frac{(N+1)(N+2)}{2}}z^N.
\end{aligned} \tag{3}$$

As far as the displacements variation along the beam axis is concerned, a one-dimensional finite element approximation is used:

$$\mathbf{u}(x, y, z) = F_\tau(y, z)\,N_i(x)\,\mathbf{q_{\tau i}} \quad \text{with} \ \tau = 1, 2, \ldots, N_u \ \text{and} \ i = 1, 2, \ldots, N_n^e \tag{4}$$

$N_i(x)$ is a C^0 shape function, N_n^e the number of nodes per element and $\mathbf{q_{\tau i}}$ the nodal displacement unknown vector. Linear, quadratic and cubic elements based on Lagrangian shape functions are considered. They are referred to as 'B2', 'B3' and 'B4', respectively.

Gemetrical and Constitutive Equations

The strain vector, ε, is grouped into a vector ε_n with components in the longitudinal direction and a vector ε_p with components laying on the cross-section planes:

$$\varepsilon_n^T = \left\{ \begin{array}{ccc} \varepsilon_{xx} & \varepsilon_{xy} & \varepsilon_{xz} \end{array} \right\}, \quad \varepsilon_p^T = \left\{ \begin{array}{ccc} \varepsilon_{yy} & \varepsilon_{zz} & \varepsilon_{yz} \end{array} \right\}. \tag{5}$$

Under the hypothesis of geometrical linearity, the strain-displacement relation is given by:

$$\begin{aligned} \varepsilon_n^T &= \left\{ \begin{array}{ccc} u_{x,x} & u_{x,y} + u_{y,x} & u_{x,z} + u_{z,x} \end{array} \right\}, \\ \varepsilon_p^T &= \left\{ \begin{array}{ccc} u_{y,y} & u_{z,z} & u_{y,z} + u_{z,y} \end{array} \right\}. \end{aligned} \tag{6}$$

Subscripts 'x', 'y' and 'z' preceded by comma mean derivation versus the corresponding coordinate. Eqs. (6) can be written in a matrix form as follows:

$$\begin{aligned} \varepsilon_n &= \mathbf{D}_{np}\mathbf{u} + \mathbf{D}_{nx}\mathbf{u}, \\ \varepsilon_p &= \mathbf{D}_p\mathbf{u}. \end{aligned} \tag{7}$$

$\mathbf{D}_{np}$, $\mathbf{D}_{nx}$, and $\mathbf{D}_p$ are the following differential matrix operators:

$$\mathbf{D}_{np} = \begin{bmatrix} 0 & 0 & 0 \\ \dfrac{\partial}{\partial y} & 0 & 0 \\ \dfrac{\partial}{\partial z} & 0 & 0 \end{bmatrix}, \quad \mathbf{D}_{nx} = \mathbf{I}\dfrac{\partial}{\partial x}, \quad \mathbf{D}_p = \begin{bmatrix} 0 & \dfrac{\partial}{\partial y} & 0 \\ 0 & 0 & \dfrac{\partial}{\partial z} \\ 0 & \dfrac{\partial}{\partial z} & \dfrac{\partial}{\partial y} \end{bmatrix} \tag{8}$$

and $\mathbf{I}$ is the unit matrix.

According to the displacement field in Eq.(4), Eqs. (7) can be written in terms of the nodal unknowns become:

$$\begin{aligned} \varepsilon_n &= \mathbf{D}_{np}F_\tau N_i \mathbf{q}_{\tau\mathbf{i}} + \mathbf{D}_{nx}F_\tau N_i \mathbf{q}_{\tau\mathbf{i}}, \\ \varepsilon_p &= \mathbf{D}_p F_\tau N_i \mathbf{q}_{\tau\mathbf{i}}. \end{aligned} \tag{9}$$

The stress vector is split coherently to what done for the strains:

$$\boldsymbol{\sigma}_p^T = \left\{ \begin{array}{ccc} \sigma_{yy} & \sigma_{zz} & \sigma_{yz} \end{array} \right\}, \quad \boldsymbol{\sigma}_n^T = \left\{ \begin{array}{ccc} \sigma_{xx} & \sigma_{xy} & \sigma_{xz} \end{array} \right\}. \tag{10}$$

In the case of a linear-elastic analysis, Hooke's law holds:

$$\boldsymbol{\sigma} = \overline{\mathbf{C}}\varepsilon, \tag{11}$$

where $\overline{\mathbf{C}}$ is the material elastic stiffness matrix. According to the used stress and strain ordering, the constitutive equations become:

$$\begin{aligned} \boldsymbol{\sigma}_p &= \overline{\mathbf{C}}_{pp}\varepsilon_p + \overline{\mathbf{C}}_{pn}\varepsilon_n, \\ \boldsymbol{\sigma}_n &= \overline{\mathbf{C}}_{np}\varepsilon_p + \overline{\mathbf{C}}_{nn}\varepsilon_n. \end{aligned} \tag{12}$$

Matrices $\overline{\mathbf{C}}_{pp}, \overline{\mathbf{C}}_{pn}, \overline{\mathbf{C}}_{np}$ and $\overline{\mathbf{C}}_{nn}$ for orthotropic materials are:

$$\overline{\mathbf{C}}_{pp} = \begin{bmatrix} \overline{C}_{22} & \overline{C}_{23} & 0 \\ \overline{C}_{23} & \overline{C}_{33} & 0 \\ 0 & 0 & \overline{C}_{44} \end{bmatrix}, \ \overline{\mathbf{C}}_{pn} = \overline{\mathbf{C}}_{np}^{T} = \begin{bmatrix} \overline{C}_{12} & \overline{C}_{26} & 0 \\ \overline{C}_{13} & \overline{C}_{36} & 0 \\ 0 & 0 & \overline{C}_{45} \end{bmatrix},$$

$$\overline{\mathbf{C}}_{nn} = \begin{bmatrix} \overline{C}_{11} & \overline{C}_{16} & 0 \\ \overline{C}_{16} & \overline{C}_{66} & 0 \\ 0 & 0 & \overline{C}_{55} \end{bmatrix}. \tag{13}$$

Coefficients $\overline{C}_{ij}$ in Eqs. (13) depend on the engineering material constants and the material orientation. Their explicit expressions can be found in Reddy [33]. Stresses are written in terms of the nodal unknowns by substituting the strain expressions in Eqs. (9) within Eqs. (12):

$$\boldsymbol{\sigma}_p = \overline{\mathbf{C}}_{pp}\mathbf{D}_p F_\tau N_i \mathbf{q}_{\tau \mathbf{i}} + \overline{\mathbf{C}}_{pn} \left(\mathbf{D}_{nn} + \mathbf{D}_{np} \right) F_\tau N_i \mathbf{q}_{\tau \mathbf{i}},$$
$$\boldsymbol{\sigma}_n = \overline{\mathbf{C}}_{np}\mathbf{D}_p F_\tau N_i \mathbf{q}_{\tau \mathbf{i}} + \overline{\mathbf{C}}_{nn} \left(\mathbf{D}_{nn} + \mathbf{D}_{np} \right) F_\tau N_i \mathbf{q}_{\tau \mathbf{i}}. \tag{14}$$

Classical Euler-Bernourlli's (EBT) and Timoshenko's (TBT) elements are derived from the first-order model. In this case, a reduced Hooke law for the axial stress/strain relation should be used:

$$\sigma_{xx} = \overline{Q}_{11}\varepsilon_{xx} + \overline{Q}_{16}\varepsilon_{xy} \tag{15}$$

This is due to the fact that the kinematic field of the classical theories accounts for a rigid cross-section ($\varepsilon_{yy} = \varepsilon_{zz} = 0$) in clear discordance with the Poisson effect. This incongruence is known as Poisson's locking and it is tackled by using Eq. (15) instead of the full three dimensional Hooke equations in the normal stress components. The reduced material stiffness coefficient $\overline{Q}_{11}$ and $\overline{Q}_{16}$ are classically obtained imposing the equations in σ_{yy} and σ_{zz} in Hooke's law equal to zero. An algebraic linear system in ε_{yy} and ε_{zz} is obtained and by substituting its solution into Hooke's equations in σ_{xx}, the reduced stiffness coefficients $\overline{Q}_{11}$ and $\overline{Q}_{16}$ are derived.

In this work, no shear correction coefficient is considered, since it depends upon several parameters, such as the geometry of the cross-section (see, for instance, Cowper [34] and Murty [35]) and the main emphasis is posed on the higher-order models. Higher-order models yield a more detailed description of the shear mechanics, the in- and out-of-section deformations, the coupling of the spatial directions due to Poisson's effect and the torsional mechanics than classical models do.

Problem Weak Form

The governing equilibrium equations of the beam are derived via the principle of virtual displacements:

$$\delta \mathscr{L}_{\text{int}} = \delta \mathscr{L}_{\text{ext}}, \tag{16}$$

where $\mathscr{L}_{\text{int}}$ represents the strain energy, $\mathscr{L}_{\text{ext}}$ is the work done by the external loads and δ stands for a virtual variation.

Element stiffness matrix nucleus

According to the stress and strain vectors splitting, the virtual variation of the strain energy is:

$$\delta \mathscr{L}_{\text{int}} = \int\limits_{l^e} \int\limits_{\Omega} \left(\delta \boldsymbol{\epsilon}_n^T \boldsymbol{\sigma}_n + \delta \boldsymbol{\epsilon}_p^T \boldsymbol{\sigma}_p \right) d\Omega dx, \tag{17}$$

where l^e is the element length. When the geometrical relations in Eqs. (9), the constitutive relations in Eqs. (14) and the finite element formulation in Eq. (4) are considered, Eq. (17) reads:

$$
\begin{aligned}
\delta L_{\text{int}} = \quad & \delta \mathbf{q}_{\tau i}^T \int\limits_{l} \int\limits_{\Omega} \left\{ (\mathbf{D}_{nx} N_i)^T F_\tau \left[\overline{\mathbf{C}}_{np} \left(\mathbf{D}_p F_s \right) N_j + \overline{\mathbf{C}}_{nn} \left(\mathbf{D}_{np} F_s \right) N_j + \overline{\mathbf{C}}_{nn} F_s \left(\mathbf{D}_{nx} N_j \right) \right] \right. \\
& + (\mathbf{D}_{np} F_\tau)^T N_i \left[\overline{\mathbf{C}}_{np} \left(\mathbf{D}_p F_s \right) N_j + \overline{\mathbf{C}}_{nn} \left(\mathbf{D}_{np} F_s \right) N_j + \overline{\mathbf{C}}_{nn} F_s \left(\mathbf{D}_{nx} N_j \right) \right] \\
& + \left. (\mathbf{D}_p F_\tau)^T N_i \left[\overline{\mathbf{C}}_{pp} \left(\mathbf{D}_p F_s \right) N_j + \overline{\mathbf{C}}_{pn} \left(\mathbf{D}_{np} F_s \right) N_j + \overline{\mathbf{C}}_{pn} F_s \left(\mathbf{D}_{nx} N_j \right) \right] \right\} d\Omega \, dx \, \mathbf{q}_{sj}.
\end{aligned}
$$

This latter can be written in the following compact vector form:

$$\delta \mathscr{L}_{\text{int}} = \delta \mathbf{q}_{\tau i}^T \mathbf{K}^{\tau s i j} \mathbf{q}_{sj}. \tag{18}$$

The components of the stiffness matrix fundamental nucleus $\mathbf{K}^{\tau s i j} \in \mathbb{R}^{3 \times 3}$ are:

$$
\begin{aligned}
K_{xx}^{\tau s i j} &= I_{i,x j,x} J_{\tau s}^{11} + I_{i,x j} J_{\tau s,y}^{16} + I_{i j,x} J_{\tau,y s}^{16} + I_{ij} \left(J_{\tau,z s,z}^{55} + J_{\tau,y s,y}^{66} \right), \\
K_{xy}^{\tau s i j} &= I_{ij,x} J_{\tau,y s}^{12} + I_{i,x j,x} J_{\tau s}^{16} + I_{ij} \left(J_{\tau,y s,y}^{26} + J_{\tau,z s,z}^{45} \right) + I_{i,x j} J_{\tau s,y}^{66}, \\
K_{xz}^{\tau s i j} &= I_{ij,x} J_{\tau,z s}^{13} + I_{ij} \left(J_{\tau,z s,y}^{36} + J_{\tau,y s,z}^{45} \right) + I_{i,x j} J_{\tau s,z}^{55}, \\
K_{yx}^{\tau s i j} &= I_{i,x j} J_{\tau s,y}^{12} + I_{i,x j,x} J_{\tau s}^{16} + I_{ij} \left(J_{\tau,y s,y}^{26} + J_{\tau,z s,z}^{45} \right) + I_{ij,x} J_{\tau,y s}^{66}, \\
K_{yy}^{\tau s i j} &= I_{ij} \left(J_{\tau,y s,y}^{22} + J_{\tau,z s,z}^{44} \right) + I_{ij,x} J_{\tau,y s}^{26} + I_{i,x j} J_{\tau s,y}^{26} + I_{i,x j,x} J_{\tau s}^{66}, \\
K_{yz}^{\tau s i j} &= I_{ij} \left(J_{\tau,z s,y}^{23} + J_{\tau,y s,z}^{44} \right) + I_{ij,x} J_{\tau,z s}^{36} + I_{i,x j} J_{\tau s,z}^{45}, \\
K_{zx}^{\tau s i j} &= I_{i,x j} J_{\tau s,z}^{13} + I_{ij} \left(J_{\tau,y s,z}^{36} + J_{\tau,z s,y}^{45} \right) + I_{ij,x} J_{\tau,z s}^{55}, \\
K_{zy}^{\tau s i j} &= I_{ij} \left(J_{\tau,y s,z}^{23} + J_{\tau,z s,y}^{44} \right) + I_{i,x j} J_{\tau s,z}^{36} + I_{ij,x} J_{\tau,z s}^{45}, \\
K_{zz}^{\tau s i j} &= I_{ij} \left(J_{\tau,z s,z}^{33} + J_{\tau,y s,y}^{44} \right) + I_{ij,x} J_{\tau,y s}^{45} + I_{i,x j} J_{\tau s,y}^{45} + I_{i,x j,x} J_{\tau s}^{55}.
\end{aligned}
\tag{19}
$$

$J_{\tau_{(,\phi)} s_{(,\xi)}}^{gh}$ is a cross-section moment and it stands for:

$$J_{\tau_{(,\phi)} s_{(,\xi)}}^{gh} = \int\limits_{\Omega} \overline{C}_{gh} F_{\tau_{(,\phi)}} F_{s_{(,\xi)}} \, d\Omega. \tag{20}$$

It is a weighted sum (in the continuum) of each elemental cross-section area where the weight functions account for the spatial distribution of the geometry and the material. $I_{i_{(,x)} j_{(,x)}}$ is an integral over the axial

coordinate of the product of the shape functions or their derivatives:

$$I_{i_{(,x)}j_{(,x)}} = \int_{l^e} N_{i_{(,x)}} N_{j_{(,x)}} \, dx. \tag{21}$$

These integrals are evaluated numerically through Gauss' quadrature method. In order to correct the shear locking, a selective integration technique is used. The selected under-integrated term is I_{lj} in $K_{uuxx}^{\tau sij}$ that is related to shear deformations γ_{xy} and γ_{xz}.

Once the approximation order N and the number of nodes per element N_n^e are fixed, the stiffness matrix of the selected element is obtained straightforwardly via summation of the previous nucleus corresponding to each term of the expansion.

Element load vector nucleus

The virtual variation of the external work given by a generic surface loading p_{ij} and a line loading l_{ij} is:

$$\delta\mathscr{L}_{\text{ext}} = \delta\mathscr{L}_{\text{ext}}^{p_{ij}} + \delta\mathscr{L}_{\text{ext}}^{l_{ij}} \tag{22}$$

The following contributes are considered for $\delta\mathscr{L}_{\text{ext}}^{p_{ij}}$:

$$\delta\mathscr{L}_{\text{ext}}^{p_{ij}} = \delta\mathscr{L}_{\text{ext}}^{p_{zz}} + \delta\mathscr{L}_{\text{ext}}^{p_{zx}} + \delta\mathscr{L}_{\text{ext}}^{p_{zy}} + \delta\mathscr{L}_{\text{ext}}^{p_{yy}} + \delta\mathscr{L}_{\text{ext}}^{p_{yx}} + \delta\mathscr{L}_{\text{ext}}^{p_{yz}}, \tag{23}$$

where:

$$\begin{aligned}
\delta\mathscr{L}_{\text{ext}}^{p_{zx}} &= \delta q_{xi\tau} I_i^{p_{zx}} E_\tau^{\overline{z}}, \quad \delta\mathscr{L}_{\text{ext}}^{p_{yx}} = \delta q_{xi\tau} I_i^{p_{yx}} E_\tau^{\overline{y}}, \\
\delta\mathscr{L}_{\text{ext}}^{p_{yy}} &= \delta q_{yi\tau} I_i^{p_{yy}} E_\tau^{\overline{y}}, \quad \delta\mathscr{L}_{\text{ext}}^{p_{zy}} = \delta q_{yi\tau} I_i^{p_{zy}} E_\tau^{\overline{z}}, \\
\delta\mathscr{L}_{\text{ext}}^{p_{zz}} &= \delta q_{zi\tau} I_i^{p_{zz}} E_\tau^{\overline{z}}, \quad \delta\mathscr{L}_{\text{ext}}^{p_{yz}} = \delta q_{zi\tau} I_i^{p_{yz}} E_\tau^{\overline{y}}
\end{aligned} \tag{24}$$

with:

$$I_i^{p_{ij}} = \int_{l^e} N_i p_{ij} dx \tag{25}$$

and:

$$\begin{aligned}
E_\tau^{\overline{z}} &= \int_{\overline{y}_1}^{\overline{y}_2} F_\tau(y, \overline{z}) dy, \\
E_\tau^{\overline{y}} &= \int_{\overline{z}_1}^{\overline{z}_2} F_\tau(\overline{y}, z) dz.
\end{aligned} \tag{26}$$

Over-lined coordinates stand for the load application domain over the cross-section. The virtual external work $\delta\mathscr{L}_{\text{ext}}^{l_{ij}}$ of a line load acting on cross-section coordinates $(\hat{y}, \hat{z})$ is:

$$\delta\mathscr{L}_{\text{ext}}^{l_{ij}} = \delta\mathscr{L}_{\text{ext}}^{l_{zz}} + \delta\mathscr{L}_{\text{ext}}^{l_{zx}} + \delta\mathscr{L}_{\text{ext}}^{l_{zy}} + \delta\mathscr{L}_{\text{ext}}^{l_{yy}} + \delta\mathscr{L}_{\text{ext}}^{l_{yx}} + \delta\mathscr{L}_{\text{ext}}^{l_{yz}}, \tag{27}$$

where:

$$\begin{aligned}
\delta\mathscr{L}_{\text{ext}}^{l_{zx}} &= \delta q_{xi\tau} I_i^{l_{zx}} F_\tau(\hat{y}, \hat{z}), \quad \delta\mathscr{L}_{\text{ext}}^{l_{yx}} = \delta q_{xi\tau} I_i^{l_{yx}} F_\tau(\hat{y}, \hat{z}), \\
\delta\mathscr{L}_{\text{ext}}^{l_{yy}} &= \delta q_{yi\tau} I_i^{l_{yy}} F_\tau(\hat{y}, \hat{z}), \quad \delta\mathscr{L}_{\text{ext}}^{l_{zy}} = \delta q_{yi\tau} I_i^{l_{zy}} F_\tau(\hat{y}, \hat{z}), \\
\delta\mathscr{L}_{\text{ext}}^{l_{zz}} &= \delta q_{zi\tau} I_i^{l_{zz}} F_\tau(\hat{y}, \hat{z}), \quad \delta\mathscr{L}_{\text{ext}}^{l_{yz}} = \delta q_{zi\tau} I_i^{l_{yz}} F_\tau(\hat{y}, \hat{z})
\end{aligned} \tag{28}$$

and:

$$I_i^{l_{ij}} = \int_{l^e} N_i l_{ij} dx. \tag{29}$$

Numerical Results

The beam support is $[0, l] \times [-b/2, b/2] \times [-h/2, h/2]$ where l is the length, h the thickness and b the width. The faces thickness is denoted by h_f. Beam geometry is presented in Fig. 1. Slender and very short beams (length-to-side ratio l/h equal to 100 and 5, respectively) are considered. The cross-section is square with thickness and width equal to 0.01 m. The ratio between skin thickness (h_f) and the total one is 0.1. The face sheets and the core of the sandwich beam are both made of aluminium. The material properties for the face sheets are: $E_f = 69$ GPa and $\nu_f = 0.33$. The core is made of hexagonal cells with a nominal size $\phi = 6.4 \cdot 10^{-3}$ m and a thickness $t = 80 \cdot 10^{-6}$ m. It is modelled as a single solid layer of an equivalent orthotropic material whose mechanical properties are given by the analytical expressions provided by Gibson and Ashby [36] and Grediac [37]. The equivalent mechanical properties are: $E_{c1} = E_{c2} = 1.62$ MPa, $E_{c3} = 2.3$ GPa, $\nu_{c12} = 0.99$, $\nu_{c13} = \nu_{c23} = 2.32 \cdot 10^{-4}$, $G_{c12} = 0.97$ MPa, $G_{c13} = 499$ MPa and $G_{c23} = 324$ MPa. Simply supported and clamped-clamped boundary conditions are considered. Beams are subjected to a surface load (bending behaviour) or an off-centric line load inducing bending and torsion as well as localised effects.

In order to validate the three-dimensional results provided by the presented one-dimensional formulation, three-dimensional finite element solutions obtained by the commercial software Ansys are used for comparison. Tri-quadratic 20-node elements "Solid186" are used. Two different meshes (a coarse and a refined one) are considered for the Ansys solution. They are referred to as 'FEM 3D-C' and 'FEM 3D-R', respectively. As far as the computational costs are concerned, the number of degrees of freedom (DOFs) for the most refined three-dimensional model (a $192 \times 48 \times 48$ mesh) are about $5.5 \cdot 10^6$. DOFs' number (N_{DOFs}) of the present one-dimensional finite elements is function of the expansion order N and the total number of nodes N_n:

$$N_{DOFs} = 3 \cdot \frac{(N+1)(N+2)}{2} \cdot N_n \tag{30}$$

In the case of the most refined model used in the analysis (a 19th-order approximation and 373 nodes) N_{DOFs} is equal to about $2.3 \cdot 10^5$.

Beams under a bending surface load

A uniform unitary pressure $p_{zz} = 1 \ Pa$ acting at $z = h/2$ and $y \in [-b/2, b/2]$ is considered. Simply supported beams are first investigated. As a first analysis, the convergence of the strain energy versus the number of nodes is studied. The results obtained via the finite element method are assessed towards an exact Navier-type solution within the framework of the present unified formulation, see Carrera and Giunta [38]. Fig. 2 shows the relative strain energy error:

$$\Delta_E = \frac{\mathscr{L}_{\text{int}}^{\text{Nav}} - \mathscr{L}_{\text{int}}^{\text{FEM}}}{\mathscr{L}_{\text{int}}^{\text{Nav}}} \tag{31}$$

versus the dimensionless distance between two consecutive nodes δ_{ii+1}/l for linear, quadratic and cubic elements. The presented results have been obtained for $N = 2$ and $l/h = 10$. Solutions for different

expansion orders and length-to-side ratios are very similar. Unless differently stated, N_n equal to 121 (corresponding to $\delta_{ii+1}/l = 0.008\overline{3}$) is assumed for all the remaining investigations since it ensures a good compromise between accuracy and computational costs.

In order to demonstrate that the proposed one-dimensional finite elements are locking-free, the variation of $\hat{u}_z$:

$$\hat{u}_z = \frac{u_z^{\text{FEM}}}{u_z^{\text{Nav}}} \tag{32}$$

computed at $(x/l, y/b, z/h) = (1/2, 0, 0)$ via B2 elements versus l/h is presented in Fig. 3. Selective and full integration strategies are compared. It can be clearly seen that the former is free of locking. Results show that this strategy is effective in correcting the locking regardless the beam theory order N.

As far as tabular results are concerned, the following displacements and stresses:

$$\tilde{u}_x = u_x\left(0, \frac{a}{2}, \frac{b}{2}\right) \quad \tilde{u}_y = u_y\left(\frac{l}{2}, \frac{a}{2}, \frac{b}{2}\right) \quad \tilde{u}_z = u_z\left(\frac{l}{2}, 0, \frac{b}{2}\right)$$

$$\tilde{\sigma}_{xx} = \sigma_{xx}\left(\frac{l}{2}, \frac{a}{2}, \frac{b}{2}\right) \quad \tilde{\sigma}_{xz} = \sigma_{xz}\left(0, \frac{a}{4}, \frac{b}{4}\right) \quad \tilde{\sigma}_{xy} = \sigma_{xy}\left(0, \frac{a}{4}, -\frac{b}{2}\right) \tag{33}$$

are accounted for. Table 2 shows the displacement components for a slender beam. One-dimensional theories with N as low as 2 yield results with a relative difference lower than 0.8% on the most relevant displacement components u_x and u_z, when compared to the three-dimensional solution. These displacements are well predicted also by Euler-Bernoulli's and Timoshenko's theories. Relative differences as high as 4.4% are obtained for the through-the-width secondary displacement u_y, that is due to Poisson effect. Displacements in the case of a very short beam are presented in Table 3. Classical EBT and TBT yield inaccurate results, being the error in the through-the-thickness component higher than 60%. Higher-order theories ($N = 19$) yield values with relative differences as high as 3.3%. Table 4 shows the stress components for a very short beam. A 19th-order one-dimensional theory yields relative differences lower than 1.2% on the relevant axial and shear stresses σ_{xx} and σ_{xz}. A relative difference of 5.4% is obtained on the secondary shear stress σ_{xy}. Stress relative differences in the case of slender beam are lower than 1.5%. The last case is not reported for the sake of brevity.

Clamped-clamped beams are now considered. After a convergence analysis, a number of nodes N_n equal to 205 and 373 has been chosen for short and slender beam analyses, respectively. The following displacements and stresses are considered:

$$\tilde{u}_x = u_x\left(\frac{l}{4}, \frac{a}{2}, \frac{b}{2}\right) \quad \tilde{u}_y = u_y\left(\frac{l}{2}, \frac{a}{2}, \frac{b}{2}\right) \quad \tilde{u}_z = u_z\left(\frac{l}{2}, 0, \frac{b}{2}\right)$$

$$\tilde{\sigma}_{xx} = \sigma_{xx}\left(\frac{l}{2}, \frac{a}{2}, \frac{b}{2}\right) \quad \tilde{\sigma}_{xz} = \sigma_{xz}\left(\frac{l}{4}, \frac{a}{4}, \frac{b}{4}\right) \quad \tilde{\sigma}_{xy} = \sigma_{xy}\left(\frac{l}{4}, \frac{a}{4}, -\frac{b}{2}\right) \tag{34}$$

Displacement components for a slender beam are presented in Table 5. Relative differences smaller than 0.5%, at worst, are obtained with N as low as 10 for u_x and u_z. The relative difference is 2.2% for u_y. Table 6 presents the displacements for a very short beam. Higher-order theories ($N \geq 16$) should be used in order to obtain relative differences lower than 5.0%. Stress components for a very short beam are

presented in Table 7. 19th-order cubic finite elements yield stress relative differences of 3.4% at worst. 3.5% difference is obtained for a slender beam. Figs. 4 and 5 present the variation of the displacement components u_x and u_y over the cross-section in the form of colour maps for a very short beam. Results provided by the three-dimensional solution are compared with those obtained with a $N = 19$ theory. The axial location of the cross-section of each component corresponds to the position of its maximum value. Stresses σ_{xx} and σ_{xy} are presented in Figs. 6 and 7. Stress results are evaluated at an opportune distance from the clamped end where, as it is well known, stress singularities are present. A $N = 19$ four-node element has been considered and a good prediction of the stress field is obtained.

Beams under a bending torsion line load

A uniform off-centric unitary line load $l_{zz} = -1 \ N/m$ acting at $(y, z) = (-b/2, h/2)$ is considered to investigate a bending/torsion solicitation. Displacements in a very short simply supported beam are presented in Table 8. A 19th-order theory yields values with relative difference being about 3.3%, at worst. A relative difference of 0.1% on the main displacements u_x and u_z and about 4.7% on the secondary displacement u_y is obtained in the case of slender beams. Stress components are shown in Table 9. A 19th-order one-dimensional theory and cubic elements yield results with a relative difference lower than 3.2% on σ_{xx} and σ_{xy}. A relative difference being about 7% is obtained on the shear stress σ_{xz}. Displacements for a very short clamped-clamped beam are presented in Table 10. A theory with $N = 19$ yields a relative difference of about 4% in the worst case. Stress components are presented in Table 11 . Stresses differ by about 5.6%, at worst. Figs. 8 to 10 present the variation of the displacement components over the cross-section in the form of colour maps for a very short beam. Stresses σ_{xx} and σ_{xy} are presented in Figs. 11 and 12. Results fairly match the reference three-dimensional FEM solution.

Comparison with experimental results

In this section, the load-displacement response provided by the presented formulation is compared with experimental results reported in [39]. Kim and Swanson [39] carried out a three-point bending test on a sandwich beam made of carbon/epoxy skins and polyurethane foam core. Hysol EA 9309NA adhesive was used to bond the foam panel to the face sheets. The investigated beam has a span length of 152.4 mm, face thickness of 0.526 mm, core thickness equal to 6.35 mm and width equal to 25.4 mm. The material properties for face sheets and core are, respectively: $E_f = 68300$ MPa, $\nu_f = 0.05$, $E_c = 72$ MPa, $\nu_c = 0.3$ and $G_c = 23.2$ MPa. Fig. 13 shows the comparison of the experimental load-displacement response with results obtained via one-dimensional $N = 19$ theory (cubic elements, 121 nodes), FEM 3D (40x24x24 elements) and Timoshenko beam theory. The displacement is evaluated at the center of the cross-section. A good correlation between UF-based one dimensional finite element solution and the linear path of the experimental response is found.

Conclusions

A family of one-dimensional finite elements has been derived through a unified formulation and it has been used for the static analysis of three-dimensional sandwich beam structures. Within this approach, the displacement field is general regardless the approximation order over the beam cross-section. Shear deformation, in- and out-of-plane warping and localised effects are all included in the formulation. Slender and very short beams have been investigated for both simply supported and clamped-clamped

boundary conditions. Surface and line loads have been accounted for. Results have been validated through comparison with three-dimensional FEM solutions obtained via the commercial code Ansys and experimental results available in the literature. Sandwich beams present a complex stress state due to the high difference in stiffness between face-sheets and core. In comparison with previous studies on isotropic, laminated and functionally graded beams by means of the same finite element formulation (see Giunta et al. [40], De Pietro et al. [41]), a reduced accuracy of results is observed for sandwich beams, due to the limits of an equivalent single layer approach in modelling such structures. Nevertheless, the presented numerical investigations have demonstrated that the relative errors on the displacements and stresses can be as high as 5% and 7%, respectively, for all the considered load and constraint configurations. A fair prediction of the static response of three-dimensional sandwich structures can, therefore, be obtained by the proposed family of UF-based one-dimensional finite elements with major advantages in terms of computational cost. Future work consists in the implementation of a family of one-dimensional finite elements based upon a layerwise approach.

Acknowledgements

References

[1] W. Fairbairn. *An account of the construction of the Britania and Conway tubular bridges*. John Weale, London, 1849.

[2] H.G. Allen. Analysis and design of structural sandwich panels. *Pergamon Press*, 1969.

[3] A. K. Noor, W. S. Burton, and C. W. Bert. Computational models for sandwich panels and shells. *Applied Mechanics Reviews*, 49(3):155–199, 1996.

[4] L. Librescu and T. Hause. Recent developments in the modeling and behavior of advanced sandwich constructions: a survey. *Composite Structures*, 48(1):1–17, 2000.

[5] D. Krajcinovic. Sandwich beam analysis. *Journal of Applied Mechanics*, 39(3):773–778, 1972.

[6] J. R. Banerjee and A. J. Sobey. Dynamic stiffness formulation and free vibration analysis of a three-layered sandwich beam. *International Journal of Solids and Structures*, 42(8):2181–2197, 2005.

[7] A. R. Damanpack and S. M. R. Khalili. High-order free vibration analysis of sandwich beams with a flexible core using dynamic stiffness method. *Composite Structures*, 94(5):1503–1514, 2012.

[8] L. Léotoing, S. Drapier, and A. Vautrin. Nonlinear interaction of geometrical and material properties in sandwich beam instabilities. *International Journal of Solids and Structures*, 39(13-14):3717–3739, 2002.

[9] Y. Frostig, M. Baruch, O. Vilnay, and I. Sheinman. High-order theory for sandwich-beam behavior with transversely flexible core. *Journal of Engineering Mechanics*, 118(5):1026–1043, 1992.

[10] Y. Frostig and Y. Shenhar. High-order bending of sandwich beams with a transversely flexible core and unsymmetrical laminated composite skins. *Composites Engineering*, 5(4):405–414, 1995.

[11] Y. B. Cho and R. Averill. An improved theory and finite-element model for laminated composite and sandwich beams using first-order zig-zag sublaminate approximations. *Composite Structures*, 37(3):281–298, 1997.

[12] S. Kapuria, P. C. Dumir, and N.K. Jain. Assessment of zigzag theory for static loading, buckling, free and forced response of composite and sandwich beams. *Composite Structures*, 64(3–4):317–327, 2004.

[13] G. M. Dai and W. H. Zhang. Size effects of basic cell in static analysis of sandwich beams. *International Journal of Solids and Structures*, 45(9):2512–2533, 2008.

[14] P Vidal and O. Polit. Vibration of multilayered beams using sinus finite elements with transverse normal stress. *Composite Structures*, 92:1524–1534, 2010.

[15] H. Hu, S. Belouettar, M. Potier-Ferry, A. Makradi, and Y. Koutsawa. Assessment of various kinematic models for instability analysis of sandwich beams. *Engineering Structures*, 33(2):572–579, 2011.

[16] H. Hu, S. Belouettar, M. Potier-Ferry, and A. Makradi. A novel finite element for global and local buckling analysis of sandwich beams. *Composite Structures*, 90(3):270–278, 2009.

[17] C. N. Phan, Y. Frostig, and G. A. Kardomateas. Analysis of sandwich beams with a compliant core and with in-plane rigidity-extended high-order sandwich panel theory versus elasticity. *Journal of Applied Mechanics*, 79(4):041001, 2012.

[18] Y. Wang and X. Wang. Static analysis of higher order sandwich beams by weak form quadrature element method. *Composite Structures*, 116:841–848, 2014.

[19] Y. Pourvais, P. Asgari, A. R. Moradi, and O. Rahmani. Experimental and finite element analysis of higher order behaviour of sandwich beams using digital projection moiré. *Polymer Testing*, 38:7–17, 2014.

[20] L. Bardella and O. Mattei. On explicit analytic solutions for the accurate evaluation of the shear stress in sandwich beams with a clamped end. *Composite Structures*, 112:157–168, 2014.

[21] S. Salami Jedari, S. Dariushi, M. Sadighi, and M. Shakeri. An advanced high-order theory for bending analysis of moderately thick faced sandwich beams. *European Journal of Mechanics-A/Solids*, 56:1–11, 2016.

[22] E. Carrera. Theories and finite elements for multilayered plates and shells: a unified compact formulation with numerical assessment and benchmarking. *Archives of Computational Methods in Engineering*, 10(3):216–296, 2003.

[23] E. Carrera and G. Giunta. Hierarchical models for failure analysis of plates bent by distributed and localized transverse loadings. *Journal of Zhejiang University SCIENCE A*, 9(5):600–613, 2008.

[24] E. Carrera and G. Giunta. Exact, hierarchical solutions for localised loadings in isotropic, laminated and sandwich shells. *Journal of Pressure Vessel Technology*, 131(4):0412021–04120214, 2009.

[25] G. Giunta, F. Biscani, S. Belouettar, and E. Carrera. Hierarchical modelling of doubly curved laminated composite shells under distributed and localised loadings. *Composites: Part B*, 42(4):682–691, 2011.

[26] G. Giunta, A. Catapano, and S. Belouettar. Failure indentation analysis of composite sandwich plates via hierarchical models. *Journal of Sandwich Structures and Materials*, 15(1):45–70, 2013.

[27] E. Carrera, G. Giunta, and M. Petrolo. *Beam Structures: Classical and Advanced Theories*. John Wiley and Sons, 2011.

[28] G. Giunta, N. Metla, Y. Koutsawa, and S. Belouettar. Free vibration and stability analysis of three-dimensional sandwich beams via hierarchical models. *Composites Part B: Engineering*, 47:326–338, 2013.

[29] A. Catapano, G. Giunta, S. Belouettar, and E. Carrera. Static analysis of laminated beams via a unified formulation. *Composite Structures*, 94(1):75–83, 2011.

[30] Q.Z. He, H. Hu, S. Belouettar, G. Guinta, K. Yu, Y. Liu, F. Biscani, E. Carrera, and M. Potier-Ferry. Multi-scale modelling of sandwich structures using hierarchical kinematics. *Composite Structures*, 93(9):2375–2383, 2011.

[31] G. Giunta, S. Belouettar, H. Nasser, E.H. Kiefer-Kamal, and T. Thielen. Hierarchical models for the static analysis of three-dimensional sandwich beam structures. *Composite Structures*, 133:1284–1301, 2015.

[32] K. J. Bathe. *Finite element procedures.* Prentice hall, 1996.

[33] J. N. Reddy. *Mechanics of laminated composite plates and shells. Theory and Analysis*. CRC Press, 2nd edition, 2004.

[34] G. R. Cowper. The shear co-efficient in Timoshenko beam theory. *Journal of Applied Mechanics*, 33(10):335–340, 1966.

[35] A. V. K. Murty. Analysis of short beams. *AIAA Journal*, 8(11):2098–2100, 1970.

[36] L. J. Gibson and M. F. Ashby. *Cellular solids: structure and properties*. Cambridge University Press, 1999.

[37] M. Grediac. A finite element study of the transverse shear in honeycomb cores. *International journal of solids and structures*, 30(13):1777–1788, 1993.

[38] E. Carrera and G. Giunta. Refined beam theories based on a unified formulation. *International Journal of Applied Mechanics*, 2(1):117–143, 2010.

[39] J. Kim and S. R. Swanson. Design of sandwich structures for concentrated loading. *Composite Structures*, 52(3):365–373, 2001.

[40] G. Giunta, G. De Pietro, H. Nasser, S. Belouettar, E. Carrera, and M. Petrolo. A thermal stress finite element analysis of beam structures by hierarchical modelling. *Composites Part B: Engineering*, 95:179–195, 2016.

[41] G. De Pietro, Y. Hui, G. Giunta, S. Belouettar, E. Carrera, and H. Hu. Hierarchical one-dimensional finite elements for the thermal stress analysis of three-dimensional functionally graded beams. *Composite Structures*, 153:514 – 528, 2016.

Tables

N	N_u	F_τ
0	1	$F_1 = 1$
1	3	$F_2 = y \quad F_3 = z$
2	6	$F_4 = y^2 \quad F_5 = yz \quad F_6 = z^2$
3	10	$F_7 = y^3 \quad F_8 = y^2z \quad F_9 = yz^2 \quad F_{10} = z^3$
...	...	...
N	$\frac{(N+1)(N+2)}{2}$	$F_{\frac{(N^2+N+2)}{2}} = y^N \quad F_{\frac{(N^2+N+4)}{2}} = y^{N-1}z \quad \ldots \quad F_{\frac{N(N+3)}{2}} = yz^{N-1} \quad F_{\frac{(N+1)(N+2)}{2}} = z^N$

Table 1. Mac Laurin's polynomials terms via Pascal's triangle.

	$10^8 \times \tilde{u}_x$		$10^{10} \times \tilde{u}_y$			$-10^6 \times \tilde{u}_z$	
FEM 3D-R[a]	7.4250		3.8089			4.6624	
FEM 3D-C[b]	7.4249		4.5823			4.6624	
	B2	B3, B4	B2	B3	B4	B2	B3, B4
$N = 19$	7.4200	7.4208	3.6532	3.6538	3.6534	4.6581	4.6587
$N = 16$	7.4199	7.4207	3.6530	3.6537	3.6533	4.6578	4.6584
$N = 14$	7.4189	7.4196	3.6515	3.6522	3.6518	4.6567	4.6574
$N = 10$	7.4171	7.4179	3.6478	3.6485	3.6481	4.6549	4.6556
$N = 7$	7.4138	7.4145	3.6466	3.6473	3.6469	4.6525	4.6531
$N = 5$	7.4054	7.4061	3.6395	3.6401	3.6397	4.6458	4.6464
$N = 2$	7.3939	7.3946	3.7191	3.7198	3.7194	4.6235	4.6241
TBT	7.4239	7.4244	0.0000	0.0000	0.0000	4.6420	4.6425
EBT	7.4239	7.4244	0.0000	0.0000	0.0000	4.6397	4.6402

a: Elements' number $192 \times 48 \times 48$. b: Elements' number $96 \times 24 \times 24$.

Table 2. Displacement components [m] for a slender simply supported sandwich beam under a bending pressure load.

	$10^{11} \times \tilde{u}_x$		$10^{13} \times \tilde{u}_y$			$-10^{11} \times \tilde{u}_z$		
FEM 3D-R[a]	1.1464		10.136			9.0535		
FEM 3D-C[b]	1.1464		10.136			9.0535		
	B2	B3, B4	B2	B3	B4	B2	B3	B4
$N = 19$	1.1329	1.1329	9.9977	9.9983	9.9982	8.7548	8.7551	8.7549
$N = 16$	1.1303	1.1305	9.9827	9.9834	9.9833	8.6927	8.6931	8.6931
$N = 14$	1.1254	1.1255	9.9504	9.9511	9.9511	8.5753	8.5757	8.5757
$N = 10$	1.1166	1.1167	9.8632	9.8639	9.8638	8.3659	8.3663	8.3663
$N = 7$	1.1125	1.1127	9.6898	9.6905	9.6904	8.2771	8.2775	8.2775
$N = 5$	1.0933	1.0935	9.4136	9.4143	9.4143	7.8487	7.8491	7.8491
$N = 2$	0.8948	0.8949	9.8055	9.8062	9.8062	3.4238	3.4242	3.4242
TBT	0.9280	0.9281	0.0000	0.0000	0.0000	3.4591	3.4595	3.4595
EBT	0.9280	0.9281	0.0000	0.0000	0.0000	2.9004	2.9007	2.9007

a: Elements' number $96 \times 48 \times 48$. *b*: Elements' number $48 \times 24 \times 24$.

Table 3. Displacement components [m] for a very short simply supported sandwich beam under a bending pressure load.

	$-10^{-1} \times \tilde{\sigma}_{xx}$			$-\tilde{\sigma}_{xz}$			$-10 \times \tilde{\sigma}_{xy}$		
FEM 3D-R[a]		4.4559			2.5867			4.3508	
FEM 3D-C[b]		4.4555			2.5900			4.3514	
	B2	B3	B4	B2	B3	B4	B2	B3	B4
$N = 19$	4.4690	4.4724	4.4686	2.6119	2.6176	2.6115	4.1234	4.1290	4.1175
$N = 16$	4.5125	4.5140	4.5133	2.3615	2.3668	2.3637	4.1479	4.1500	4.1470
$N = 14$	4.2891	4.2905	4.2899	2.6483	2.6536	2.6507	4.1590	4.1633	4.1573
$N = 10$	4.4153	4.4168	4.4161	3.0426	3.0474	3.0442	4.3898	4.3979	4.3981
$N = 7$	4.4918	4.4934	4.4926	2.7208	2.7266	2.7236	3.9645	3.9577	3.9302
$N = 5$	4.2262	4.2279	4.2270	2.2555	2.2610	2.2579	4.1747	4.2278	4.2414
$N = 2$	3.8392	3.8410	3.8400	0.2270	0.2287	0.2272	8.3580	8.3539	8.3720
TBT	3.8416	3.8428	3.8421	0.2212	0.2235	0.2233	0.0000	0.0000	0.0000
EBT	3.8416	3.8428	3.8421	$-^{c}$	$-$	$-$	$-$	$-$	$-$

a: Elements' number $96 \times 48 \times 48$. b: Elements' number $48 \times 24 \times 24$.

c: Result not provided by the theory.

Table 4. Stress components $\tilde{\sigma}_{xx}$, $\tilde{\sigma}_{xz}$ and $\tilde{\sigma}_{xy}$ [Pa] for a very short simply supported sandwich beam under a bending pressure load.

	$10^8 \times \tilde{u}_x$			$10^{10} \times \tilde{u}_y$			$-10^7 \times \tilde{u}_z$		
FEM 3D-R[a]		1.3923			1.2421			9.5066	
FEM 3D-C[b]		1.3923			1.2661			9.5063	
	B2	B3	B4	B2	B3	B4	B2	B3	B4
$N = 19$	1.3899	1.3952	1.3906	1.2166	1.2169	1.2171	9.4739	9.4788	9.4816
$N = 16$	1.3898	1.3951	1.3906	1.2165	1.2168	1.2170	9.4713	9.4762	9.4791
$N = 14$	1.3896	1.3949	1.3904	1.2160	1.2163	1.2165	9.4655	9.4704	9.4733
$N = 10$	1.3892	1.3945	1.3900	1.2147	1.2150	1.2152	9.4553	9.4601	9.4630
$N = 7$	1.3886	1.3939	1.3893	1.2142	1.2145	1.2147	9.4477	9.4525	9.4554
$N = 5$	1.3869	1.3922	1.3876	1.2116	1.2120	1.2121	9.4206	9.4254	9.4282
$N = 2$	1.3834	1.3886	1.3841	1.2382	1.2385	1.2387	9.2338	9.2384	9.2410
TBT	1.3921	1.3969	1.3921	0.0000	0.0000	0.0000	9.3026	9.3029	9.3029
EBT	1.3921	1.3969	1.3921	0.0000	0.0000	0.0000	9.2802	9.2805	9.2805

a: Elements' number $192 \times 48 \times 48$. b: Elements' number $96 \times 24 \times 24$.

Table 5. Displacement components [m] for a slender clamped-clamped sandwich beam under a bending pressure load.

	$10^{12} \times \tilde{u}_x$			$10^{13} \times \tilde{u}_y$			$-10^{11} \times \tilde{u}_z$		
FEM 3D-R[a]		2.8184			4.0643			6.1116	
FEM 3D-C[b]		2.8177			4.0630			6.1085	
	B2	B3	B4	B2	B3	B4	B2	B3	B4
$N = 19$	2.7583	2.7896	2.7597	3.9521	3.9530	3.9535	5.8584	5.8601	5.8610
$N = 16$	2.7469	2.7780	2.7480	3.9389	3.9399	3.9403	5.8058	5.8073	5.8082
$N = 14$	2.7247	2.7554	2.7259	3.9121	3.9131	3.9136	5.7059	5.7075	5.7083
$N = 10$	2.6854	2.7152	2.6865	3.8363	3.8373	3.8377	5.5280	5.5294	5.5302
$N = 7$	2.6694	2.6989	2.6705	3.6669	3.6679	3.6683	5.4426	5.4439	5.4446
$N = 5$	2.5889	2.6168	2.5900	3.4184	3.4194	3.4197	5.0858	5.0866	5.0868
$N = 2$	1.6781	1.6881	1.6786	3.7568	3.7574	3.7575	1.1211	1.1213	1.1213
TBT	1.7401	1.7508	1.7401	0.0000	0.0000	0.0000	1.1393	1.1393	1.1393
EBT	1.7401	1.7508	1.7401	0.0000	0.0000	0.0000	0.5805	0.5806	0.5806

a: Elements' number $96 \times 48 \times 48$. b: Elements' number $48 \times 24 \times 24$.

Table 6. Displacement components [m] for a very short clamped-clamped sandwich beam under a bending pressure load.

	$-10^{-1} \times \tilde{\sigma}_{xx}$			$-\tilde{\sigma}_{xz}$			$-10 \times \tilde{\sigma}_{xy}$		
FEM 3D-R[a]	1.9101			1.3819			1.7609		
FEM 3D-C[b]	1.9095			1.3819			1.7549		
	B2	B3	B4	B2	B3	B4	B2	B3	B4
$N = 19$	1.9150	1.9158	1.9153	1.3819	1.4215	1.3932	1.5873	1.7748	1.7018
$N = 16$	1.9428	1.9437	1.9436	1.2497	1.2862	1.2615	1.5884	1.7576	1.6541
$N = 14$	1.7572	1.7580	1.7579	1.4019	1.4412	1.4134	1.5668	1.7342	1.6321
$N = 10$	1.8889	1.8898	1.8897	1.6075	1.6505	1.6187	1.5520	1.7158	1.6167
$N = 7$	1.9352	1.9362	1.9360	1.4461	1.4857	1.4571	1.4902	1.6479	1.5540
$N = 5$	1.7581	1.7591	1.7589	1.1865	1.2202	1.1967	1.4095	1.5650	1.4737
$N = 2$	1.3391	1.3398	1.3395	0.1146	0.1186	0.1163	4.7620	4.8979	4.8066
TBT	1.2806	1.2810	1.2807	0.1099	0.1139	0.1116	0.0000	0.0000	0.0000
EBT	1.2806	1.2810	1.2807	$-^c$	$-$	$-$	$-$	$-$	$-$

a: Elements' number $96 \times 48 \times 48$. b: Elements' number $48 \times 24 \times 24$.

c: Result not provided by the theory.

Table 7. Stress components $\tilde{\sigma}_{xx}$, $\tilde{\sigma}_{xz}$ and $\tilde{\sigma}_{xy}$ [Pa] for a very short clamped-clamped sandwich beam under a bending pressure load.

	$10^9 \times \tilde{u}_x$		$-10^9 \times \tilde{u}_y$			$-10^9 \times \tilde{u}_z$	
FEM 3D-R[a]	1.7721		2.9587			8.8508	
FEM 3D-C[b]	1.7722		2.9588			8.8508	
	B2	B3, B4	B2	B3	B4	B2	B3, B4
$N = 19$	1.7415	1.7415	2.8742	2.8743	2.8744	8.5582	8.5586
$N = 16$	1.7403	1.7404	2.8767	2.8768	2.8768	8.4974	8.4978
$N = 14$	1.7295	1.7296	2.8460	2.8461	2.8461	8.3800	8.3804
$N = 10$	1.7110	1.7111	2.7931	2.7932	2.7932	8.1755	8.1759
$N = 7$	1.6679	1.6680	2.6573	2.6574	2.6574	8.0992	8.0996
$N = 5$	1.6028	1.6029	2.4457	2.4458	2.4458	7.7032	7.7036
$N = 2$	1.0423	1.0424	0.6832	0.6832	0.6832	3.4457	3.4461
TBT	0.9280	0.9281	0.0000	0.0000	0.0000	3.4591	3.4595
EBT	0.9280	0.9281	0.0000	0.0000	0.0000	2.9004	2.9007

a: Elements' number $96 \times 48 \times 48$. *b*: Elements' number $48 \times 24 \times 24$.

Table 8. Displacement components [m] for a very short simply supported sandwich beam under an off-centric line load.

	$-10^{-3} \times \tilde{\sigma}_{xx}$			$-10^{-2} \times \tilde{\sigma}_{xz}$			$10^{-3} \times \tilde{\sigma}_{xy}$		
FEM 3D-R[a]	7.2313			1.2794			2.0451		
FEM 3D-C[b]	7.2324			1.2801			2.0470		
	B2	B3	B4	B2	B3	B4	B2	B3	B4
$N = 19$	7.0062	7.0083	7.0036	1.3704	1.3690	1.3725	1.9901	1.9926	1.9908
$N = 16$	7.0818	7.0840	7.0828	1.1527	1.1519	1.1499	1.9823	1.9851	1.9836
$N = 14$	6.9644	6.9664	6.9654	1.2874	1.2921	1.2929	1.9772	1.9796	1.9794
$N = 10$	7.0709	7.0731	7.0719	1.4264	1.4314	1.4321	1.9088	1.9106	1.9087
$N = 7$	6.9556	6.9578	6.9565	1.5267	1.5324	1.5350	1.8802	1.8840	1.8832
$N = 5$	6.5607	6.5629	6.5616	1.1270	1.1245	1.1221	1.9251	1.9201	1.9163
$N = 2$	4.2154	4.2172	4.2162	0.0356	0.0328	0.0308	0.6113	0.6093	0.6092
TBT	3.8416	3.8428	3.8421	0.2212	0.2235	0.2233	0.0000	0.0000	0.0000
EBT	3.8416	3.8428	3.8421	$-^c$	—	—	—	—	—

a: Elements' number $96 \times 48 \times 48$. b: Elements' number $48 \times 24 \times 24$.

c: Result not provided by the theory.

Table 9. Stress components $\tilde{\sigma}_{xx}$, $\tilde{\sigma}_{xz}$ and $\tilde{\sigma}_{xy}$ [Pa] for a very short simply supported sandwich beam under an off-centric line load.

	$10^{10} \times \tilde{u}_x$			$-10^{9} \times \tilde{u}_y$			$-10^{9} \times \tilde{u}_z$		
FEM 3D-R^a		5.3473			1.6120			5.8759	
FEM 3D-C^b		5.3456			1.6111			5.8727	
	B2	B3	B4	B2	B3	B4	B2	B3	B4
$N = 19$	5.2398	5.2865	5.2419	1.5873	1.5878	1.5880	5.6305	5.6325	5.6331
$N = 16$	5.2307	5.2776	5.2327	1.5884	1.5889	1.5891	5.5794	5.5809	5.5818
$N = 14$	5.1921	5.2386	5.1941	1.5790	1.5796	1.5797	5.4800	5.4815	5.4824
$N = 10$	5.1232	5.1690	5.1250	1.5624	1.5629	1.5630	5.3079	5.3093	5.3101
$N = 7$	4.9961	5.0409	4.9978	1.5241	1.5245	1.5246	5.2360	5.2373	5.2380
$N = 5$	4.7642	4.8069	4.7655	1.4459	1.4462	1.4462	4.9144	4.9152	4.9154
$N = 2$	2.1132	2.1290	2.1137	0.5410	0.5410	0.5410	1.1148	1.1151	1.1151
TBT	1.7401	1.7508	1.7401	0.0000	0.0000	0.0000	1.1393	1.1393	1.1393
EBT	1.7401	1.7508	1.7401	0.0000	0.0000	0.0000	0.5805	0.5806	0.5806

a: Elements' number $96 \times 48 \times 48$. b: Elements' number $48 \times 24 \times 24$.

Table 10. Displacement components [m] for a very short clamped-clamped sandwich beam under an off-centric line load.

	$-10^{-3} \times \tilde{\sigma}_{xx}$			$-10^{-1} \times \tilde{\sigma}_{xz}$			$10^{-2} \times \tilde{\sigma}_{xy}$		
FEM 3D-R[a]		3.7175			9.9206			10.126	
FEM 3D-C[b]		3.7192			9.9214			10.132	
	B2	B3	B4	B2	B3	B4	B2	B3	B4
$N = 19$	3.5135	3.5129	3.5083	10.086	10.445	10.154	9.8592	10.1940	9.9967
$N = 16$	3.6194	3.6210	3.6208	8.8559	9.1464	8.9525	9.8497	10.182	9.9808
$N = 14$	3.5605	3.5621	3.5619	9.8799	10.191	9.9743	9.8181	10.149	9.9487
$N = 10$	3.6506	3.6523	3.6519	11.169	11.507	11.260	9.6825	10.010	9.8122
$N = 7$	3.6239	3.6255	3.6251	10.656	10.978	10.747	9.4915	9.8162	9.6192
$N = 5$	3.4314	3.4330	3.4324	8.2948	8.5636	8.3791	9.3204	9.6422	9.4456
$N = 2$	1.4695	1.4703	1.4700	0.3778	0.3994	0.3894	3.6036	3.7375	3.6562
TBT	1.2806	1.2810	1.2807	1.0994	1.1387	1.1164	0.0000	0.0000	0.0000
EBT	1.2806	1.2810	1.2807	$-^c$	$-$	$-$	$-$	$-$	$-$

a: Elements' number $96 \times 48 \times 48$. b: Elements' number $48 \times 24 \times 24$.

c: Result not provided by the theory.

Table 11. Stress components $\tilde{\sigma}_{xx}$, $\tilde{\sigma}_{xz}$ and $\tilde{\sigma}_{xy}$ [Pa] for a very short clamped-clamped sandwich beam under an off-centric line load.

Figures
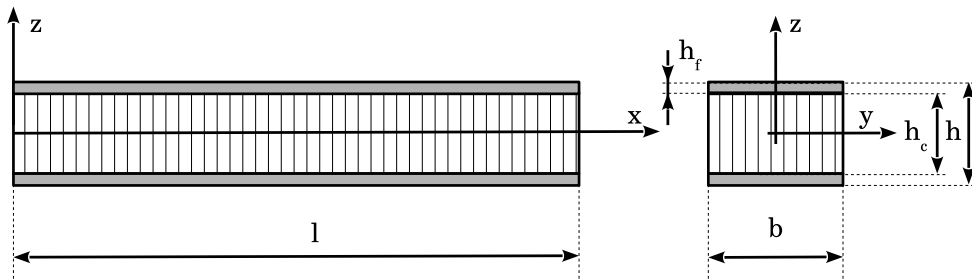
Figure 1. Sandwich beam configuration.
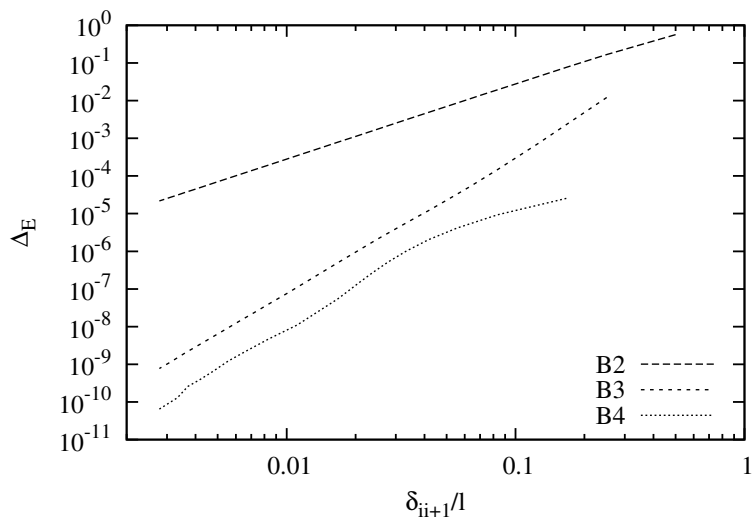
Figure 2. Relative strain energy error (with reference to Navier closed form solution) versus the dimensionless distance between two consecutive nodes, $N = 2$, $l/h = 10$, simply supported sandwich beam under pressure load p_{zz}.
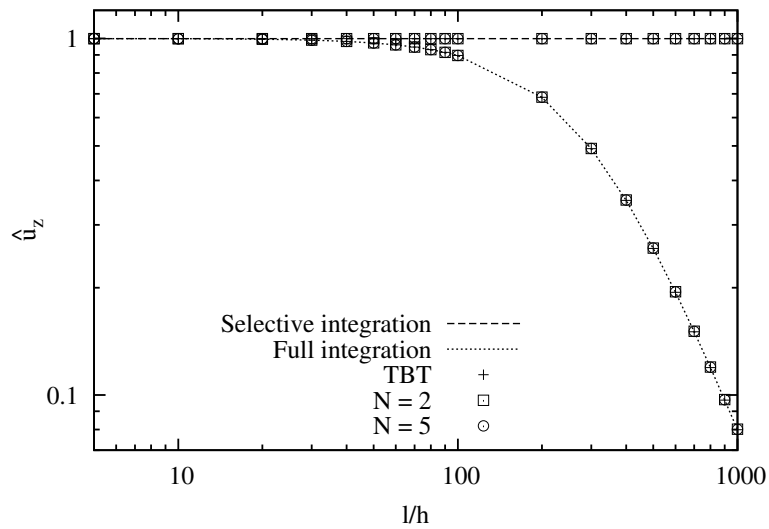
Figure 3. Shear locking correction via selective integration for B2 element, simply supported sandwich beam, pressure load.
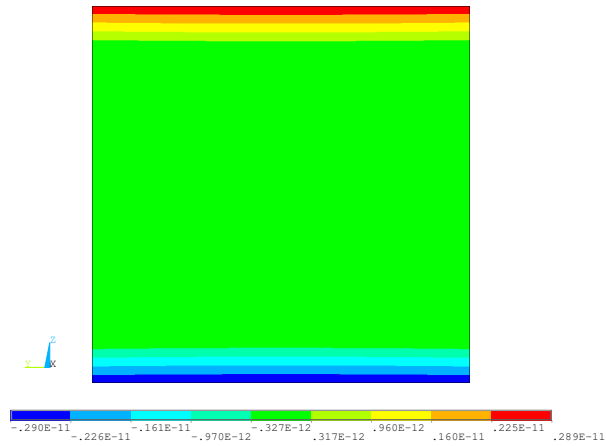
(a)
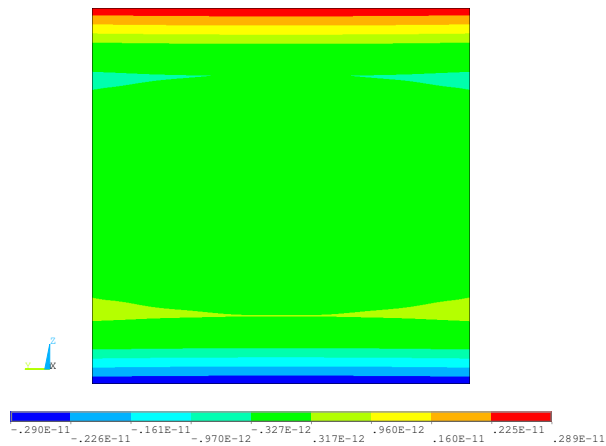
(b)

Figure 4. Axial displacement u_x [m] over the cross-section at $x = l/4$ via (a) FEM 3D-R solution and (b) $N = 19$ B4 model for $l/h = 5$, very short clamped-clamped beam under bending surface load.
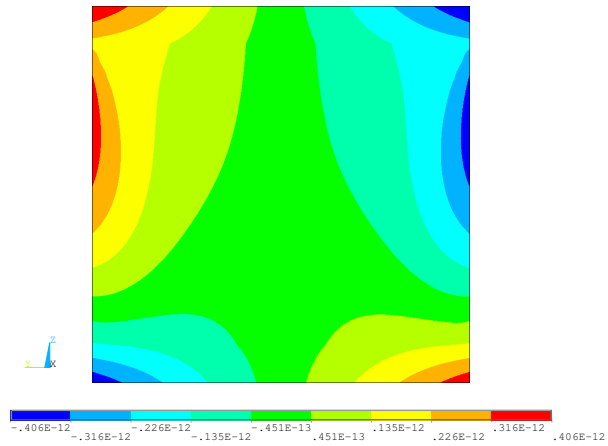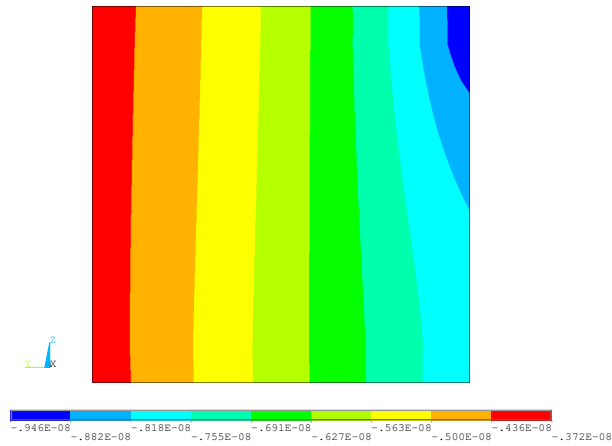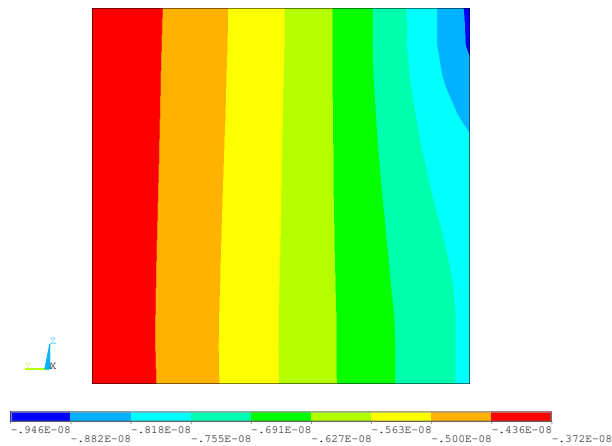
(a)
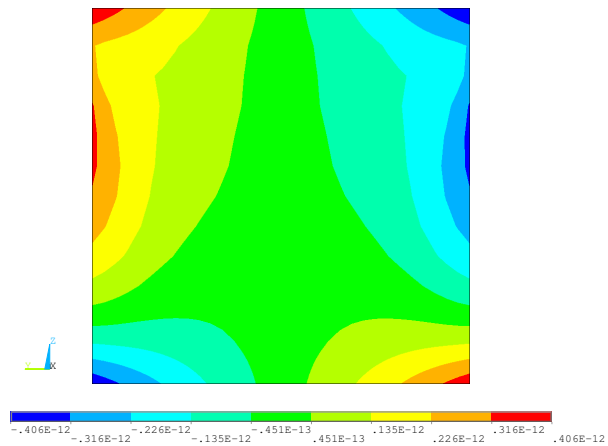
(b)

Figure 5. Through-the-width displacement u_y [m] over the cross-section at $x = l/2$ via (a) FEM 3D-R solution and (b) $N = 19$ B4 model for $l/h = 5$, very short clamped-clamped beam under bending surface load.
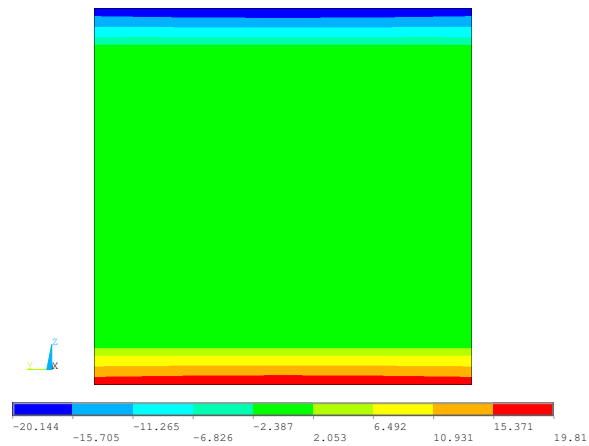
(a)
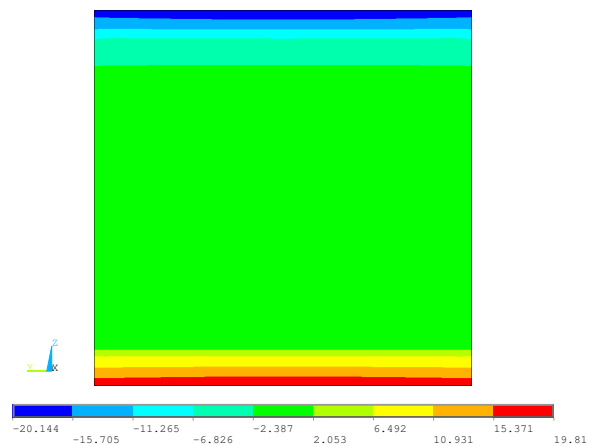
(b)

Figure 6. Axial stress σ_{xx} [Pa] over the cross-section at $x = l/2$ via (a) FEM 3D-R solution and (b) $N = 19$ B4 model for $l/h = 5$, very short clamped-clamped beam under bending surface load.
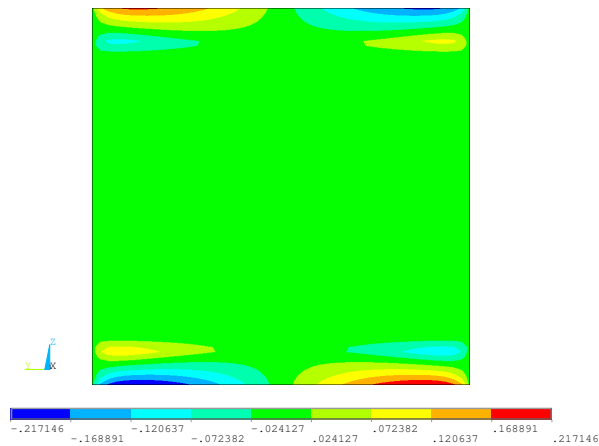
(a)
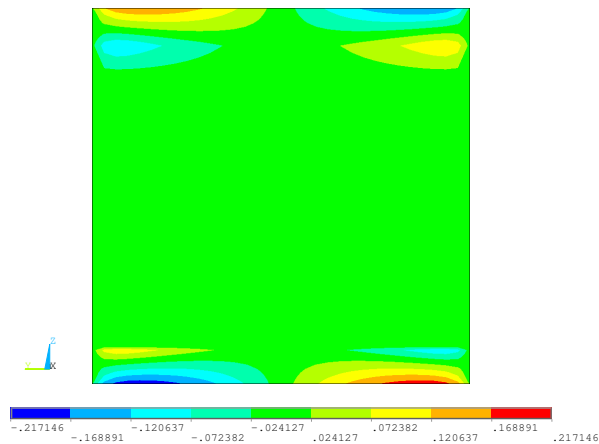
(b)

Figure 7. Shear stress σ_{xy} [Pa] over the cross-section at $x = l/4$ via (a) FEM 3D-R solution and (b) $N = 19$ B4 model for $l/h = 5$, very short clamped-clamped beam under bending surface load.
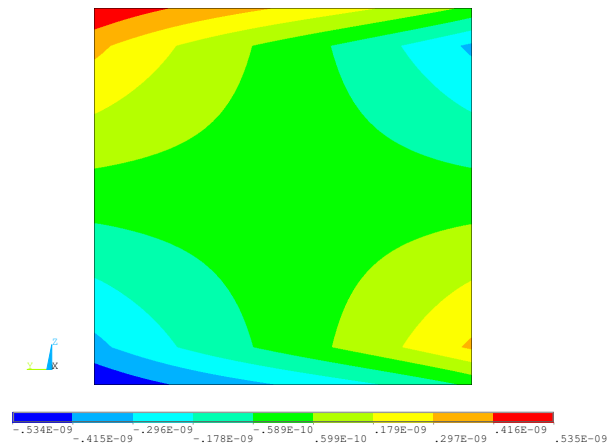
(a)
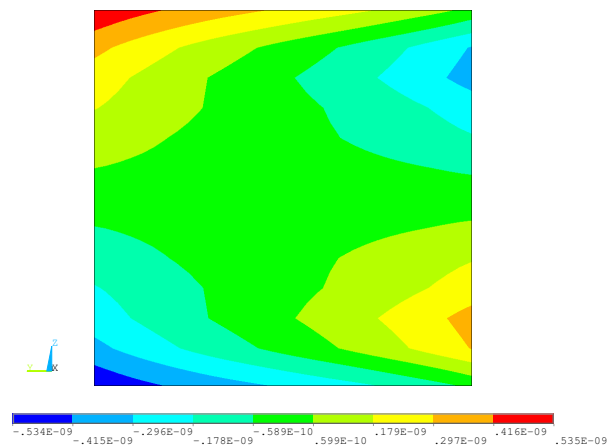
(b)

Figure 8. Axial displacement u_x [m] over the cross-section at $x = l/4$ via (a) FEM 3D-R solution and (b) $N = 19$ B4 model for $l/h = 5$, very short clamped-clamped beam under an off-centric line load.
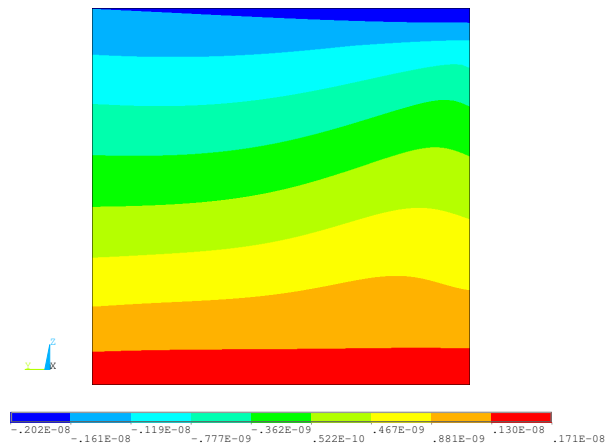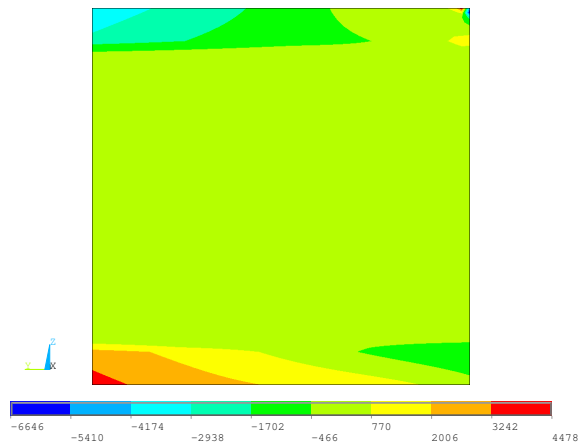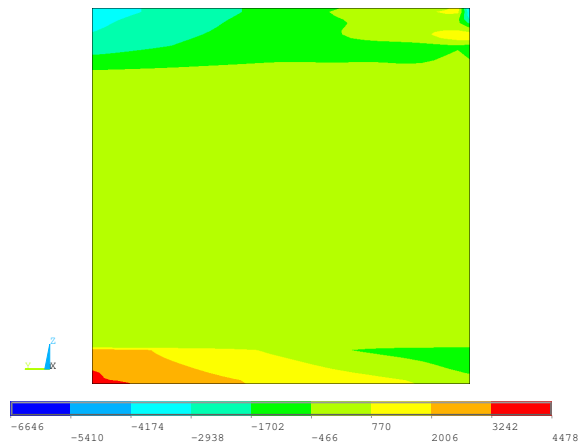
(a)
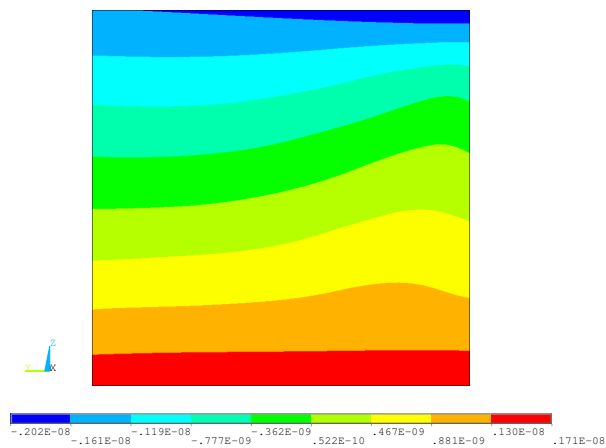
(b)

Figure 9. Through-the-width displacement u_y [m] over the cross-section at $x = l/2$ via (a) FEM 3D-R solution and (b) $N = 19$ B4 model for $l/h = 5$, very short clamped-clamped beam under an off-centric line load.
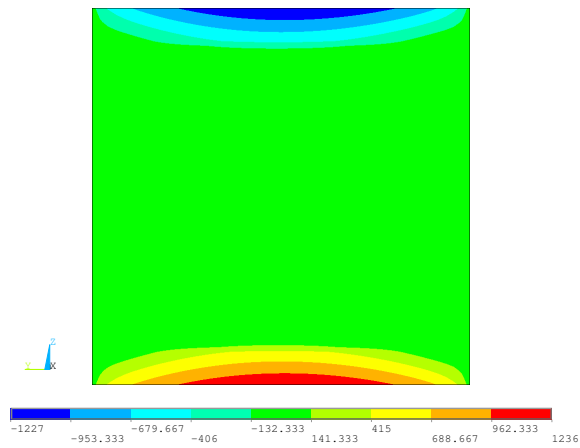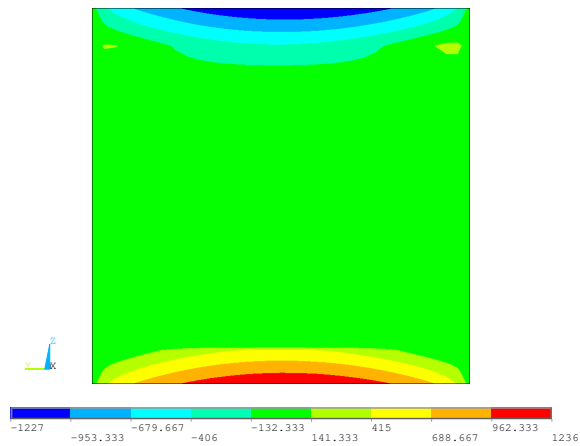
(a)

(b)

Figure 10. Through-the-thickness displacement u_z [m] over the cross-section at $x = l/2$ via (a) FEM 3D-R solution and (b) $N = 19$ B4 model for $l/h = 5$, very short clamped-clamped beam under an off-centric line load.

(a)

(b)

Figure 11. Axial stress σ_{xx} [Pa] over the cross-section at $x = l/2$ via (a) FEM 3D-R solution and (b) $N = 19$ B4 model for $l/h = 5$, very short clamped-clamped beam under an off-centric line load.

(a)

(b)

Figure 12. Shear stress σ_{xy} [Pa] over the cross-section at $x = l/4$ via (a) FEM 3D-R solution and (b) $N = 19$ B4 model for $l/h = 5$, very short clamped-clamped beam under an off-centric line load.
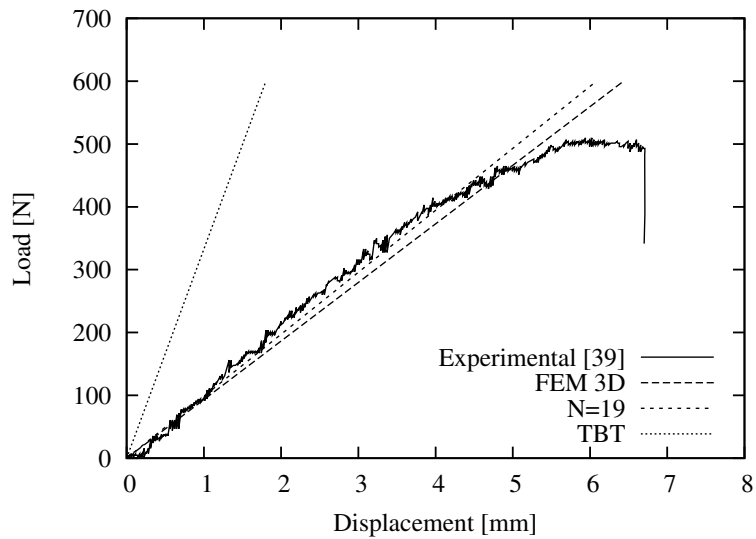
Figure 13. Load-displacement response for three-point bending test of a sandwich beam with carbon/epoxy faces and polyurethane foam core.